

Repulsion between calcite crystals and grain detachment during water–rock interaction

Y. Levenson¹, S. Emmanuel^{1*}



doi: 10.7185/geochemlet.1714

Abstract

Weathering in carbonate rocks is often thought to be governed by chemical dissolution. However, recent studies have shown that mechanical detachment of tiny grains contributes significantly to the overall surface retreat. Whether this detachment is caused by shear forces acting at the surface, or repulsive forces acting between grains, was not known. In this study, we used atomic force microscopy to examine the mechanism of grain detachment and we demonstrate that it occurs even in the absence of shearing fluid flow. This suggests that the removal of grains from rock surfaces can be caused by repulsive forces between calcite grains. Although these repulsive forces are expected to be sensitive to the ionic strength of the solution, we did not find enough evidence to demonstrate a correlation between salinity and the frequency of grain detachment. Importantly, our findings suggest that grain detachment occurs during water–rock interaction under low flow conditions over a range of salinities, with potential impacts on geological carbon sequestration and enhanced oil recovery in carbonate formations.

Received 27 September 2016 | Accepted 9 January 2017 | Published 31 January 2017

Introduction

The geochemical interaction between carbonate rocks and reactive fluids strongly influences the way many rock formations weather. Although chemical dissolution of carbonate minerals plays a key role in weathering (Morse and Arvidson, 2002; Ford and Williams, 2007; Morse *et al.*, 2007), some studies have suggested that micrometre- and even nanometre-scale mechanical processes can be equally important (Cooper *et al.*, 1992; Vleugels and Van Grieken, 1995; Luquot *et al.*, 2014; Emmanuel *et al.*, 2015). For example, Levenson and Emmanuel (2016) recently showed that ~40 % of the mass removed during weathering experiments on fine-grained limestone is attributable to the detachment of grains

from the rock surface, a process which is preceded by chemical dissolution along grain boundaries. While those experiments were able to quantify this chemo-mechanical process, the actual mechanism that causes tiny grains to detach from the surface was unclear. Because all the experiments in which grain detachment was observed were carried out in a flowing fluid, shear forces at the solid–water interface were suggested as a possible factor (Levenson and Emmanuel, 2016). However, the frequency of grain detachment events did not increase with flow rate, hinting that shearing might not be the only mechanism influencing grain detachment.

Recently, Røyne *et al.* (2015) showed that in the presence of water, calcite grains repel each other. This process could weaken carbonate rocks. These repulsive forces are likely to be related to water adsorption on the crystal surfaces or to the electric double layer (Nara *et al.*, 2014; Røyne *et al.*, 2015) but in both cases, decreasing the concentration of dissolved ions is expected to increase the degree of repulsion. Such intergranular repulsion could be an important factor in calcite grain detachment from the surface of rocks during weathering, but whether or not repulsive forces do in fact shape reacting rock surfaces has yet to be determined.

The aim of this study was to isolate the effect of repulsive forces on grain detachment. We present the results from experiments carried out under zero flow conditions, to exclude the influence of shear forces. We also considered the impact of ionic strength and the implications of our results for rock weathering and geological carbon capture.

Methods

We used atomic force microscopy (AFM), which provides nanometre-scale resolution and *in situ* imaging in fluid environments. This technique has already been used to examine grain detachment in carbonate rocks (Emmanuel and Levenson, 2014; Levenson and Emmanuel, 2016), although in those previous studies, all experiments were carried out under constant fluid flow. Each sample was prepared from a 5.5 mm diameter core of Solnhofen micritic limestone that was embedded in a Plexiglas disk and polished with an ATM Saphir 520 single wheel grinder with a fluid polishing compound containing one-micrometre diamond particles. After polishing, the sample was rinsed with deionised water and wiped with ethanol. To create an inert datum, the samples were partially covered with a 150 nm layer of gold.

Once prepared, the sample was sealed in a fluid imaging cell on the AFM scanner (Veeco Multimode 8 AFM with a NanoScope V controller and NanoScope 8.15 software). Solutions were injected periodically into the system using a syringe pump. An initial 30 min pulse at 2 ml hr⁻¹ was followed by alternating periods of no flow, *i.e.* 0 ml hr⁻¹ (60 min), and flow at 2 ml hr⁻¹ (15 min).

1. Institute of Earth Sciences, The Hebrew University of Jerusalem, Edmond J. Safra Campus, Givat Ram, Jerusalem 91904, Israel

* Corresponding author (email: simonem@cc.huji.ac.il)



To keep the solutions undersaturated with respect to calcite during the intervals of zero flow, we used the chelating agent ethylenediaminetetraacetic acid (EDTA disodium salt dihydrate, crystal, BAKER ANALYZED® ACS Reagent) at a concentration of 2 mM in all experiments. The addition of EDTA accelerates dissolution, although it does not affect the overall dissolution mechanism (Fredd and Fogler, 1998; Oelkers *et al.*, 2011). To change the ionic strength of the solutions, we used NaCl (BAKER ANALYZED® ACS Reagent) at concentrations in the range 0–500 mM (Table S-1). The pH of the solutions was 4.7–5.1. A total of 12 experiments was carried out.

To track the evolution of the limestone surface, the sample was imaged continuously during the experiments with silicon nitride probes (Bruker ScanAsyst Fluid+). Scans of $20\ \mu\text{m} \times 20\ \mu\text{m}$ regions were performed at a line rate of 1 Hz with a resolution of 256×256 pixels using the Peakforce ScanAsyst non-contact imaging method. Two imaging modes were recorded: Peakforce Error mode, which produces a pseudo-3D image emphasising topography, and topographical mapping mode, which provides the precise height of the surface. In the data shown here, the gold surface was used as a reference to register the data in the x,y,z planes. In some cases, the surfaces of the samples were imaged at the end of the experiments using environmental scanning electron microscopy (ESEM; FEI Quanta 200).

Data analysis was carried out using ESRI ArcGIS software implementing similar methods to those described by Levenson and Emmanuel (2016). Large topographic changes between sequential scans allowed us to count grain detachment events, which were defined as regions with lateral spatial dimension >300 nm, that had undergone vertical change in topography between scans of at least 100 nm. The events were detected by subtracting the topography of the second image in the sequence from the first. The events were counted manually. While even smaller grains could detach from the surface, this threshold provided a minimum estimate for the number of events.

Results and Discussion

In each experiment, we observed a significant number of grain detachment events, both during fluid flow and during stagnant periods (Fig. 1). Grain detachment during periods of no flow indicates that fluid shear forces are not the only mechanism for removing grains from the rock surface. Because the frequency of detachment events did not increase during flow (Fig. 2), shearing could even play a minor role in grain detachment. Rather than directly dislodging grains from the surface in our experiments, flow probably replenishes the undersaturated solution in contact with the rock, thereby facilitating dissolution along grain boundaries.

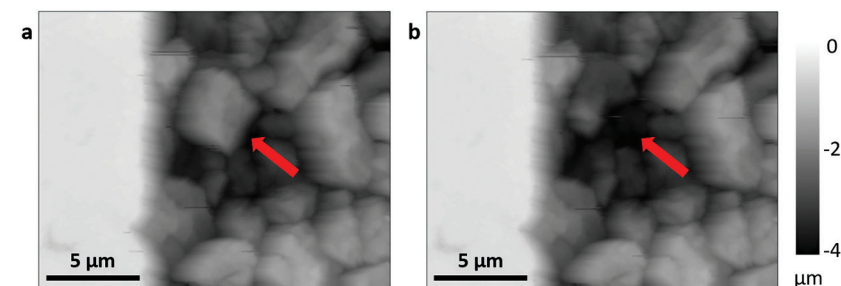


Figure 1 Topographic maps obtained using AFM (a) before and (b) after a grain detachment event (indicated by the red arrow) during zero flow. In both images, the smooth region to the left of the field was masked by gold. The experiment was carried out in a solution of 500 mM NaCl.

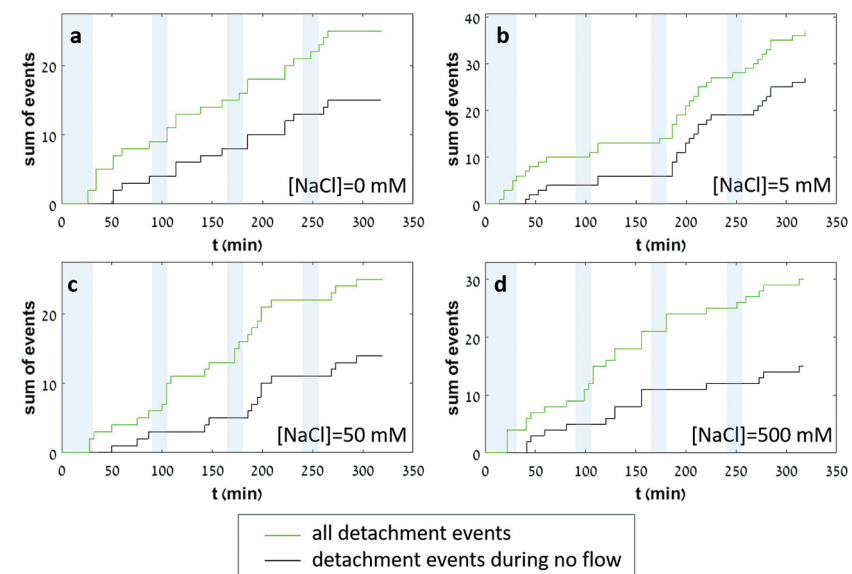


Figure 2 Cumulative grain detachment events versus time in four representative experiments carried out at different salinities. Light blue bars indicate periods of flow, while white regions indicate periods of no flow. Numerous events are observed in all the experiments during zero flow conditions.

While grain detachment was clearly seen in the experiments during periods of zero flow, it is possible that grains could be plucked from the surface as a result of attractive van der Waals forces acting between the AFM tip and



the calcite grains. Although not measured directly in this study, such forces are estimated to be on the order of 2 nN in water (Lomboy *et al.*, 2011). DVLO theory predicts that the maximum pressure resulting from double layer repulsive forces acting between surfaces in a calcite saturated fluid is 2.8 kPa (Røyne *et al.*, 2015). Thus, a calcite grain that is 1 μm in diameter, with a grain–grain contact area of 5 μm^2 , is expected to experience a repulsive force of ~ 14 nN caused by double layer repulsion. Røyne *et al.* (2015) reported repulsive pressures as high as 23 kPa, suggesting that the repulsive force for a 1- μm grain could be greater than 100 nN. Because the tip–grain force is smaller than the forces expected for grain–grain interaction, intergranular repulsive forces are likely to dominate the behaviour of micrometre-sized calcite grains. However, this comparison does not rule out the possibility that the tip affects our measurements, especially for smaller calcite particles.

To shed more light on this issue, after the experiments were terminated, we compared areas that had been scanned continuously during the experiments with areas that had not been scanned. If the AFM tip were responsible for removing grains from the surface, we would expect areas that had been scanned continuously to be rougher than regions that had not been imaged. However, we found no significant difference in the roughness (Fig. S-1), suggesting that AFM scanning does not have a major impact on the evolution of surface topography.

In addition to the roughness measurements, we also carried out five additional experiments in which regions of the limestone surface were imaged once with the AFM at the beginning of a period of zero flow. In each experiment, between 1 and 3 different regions were imaged. After an hour of no flow, the experiment was terminated and imaged with ESEM, and then scanned again with AFM under dry conditions. In 9 of the 13 scanned regions, we found examples where grains present at the beginning of the period of zero flow were absent from both the ESEM and AFM images, indicating that the grains were not removed by interaction with the AFM tip (Fig. S-2).

Repulsive forces between calcite crystals, caused by water adsorption or the electric double layer (Nara *et al.*, 2014; Røyne *et al.*, 2015), should be sensitive to the ionic strength of the solution. Specifically, increasing ionic strength is expected to decrease the repulsion between the grains and this is expected to result in a lower frequency of grain detachment events. However, in the range that we tested, there was no significant correlation between ionic strength and the frequency of grain detachment during periods of zero flow ($R^2 = 0.006$; Fig. 3). Because the AFM experiments provide a limited field of view, which results in a statistically small number of detachment events, minor effects resulting from changes in ionic strength could be masked by the relatively large variability we observe in our experiments.

Another reason for the lack of correlation between the frequency of grain detachment events and ionic strength could be related to the rate of chemical dissolution. Because grain detachment is a chemo-mechanical process, changes in the rate of dissolution at crystal surfaces and along grain boundaries would

impact the frequency of events. If increasing ionic strength were to cause the dissolution rate to *increase* and the repulsive forces to *decrease*, there might be no net change in the observed rate of grain detachment. Some studies have indicated that ionic strength influences calcite dissolution rates (Buhmann and Dreybrodt, 1987; Gledhill and Morse, 2006; Ruiz-Agudo *et al.*, 2010). However, in the salinity range that we tested, we found no significant effect ($R^2 = 0.16$; Fig. 4) but this could be a result of the far from equilibrium conditions in our experiments.

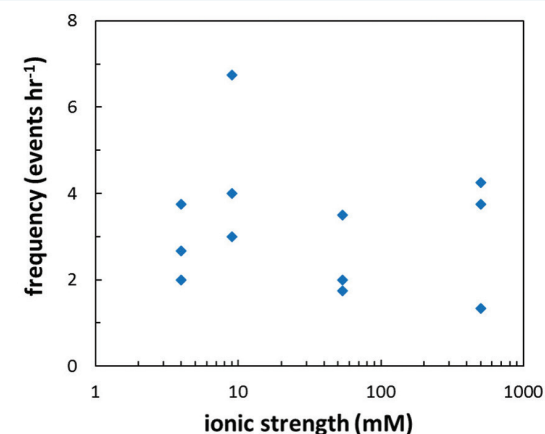


Figure 3 Frequency of grain detachment events during zero flow versus the ionic strength of the solution. There is no significant correlation between the two parameters.

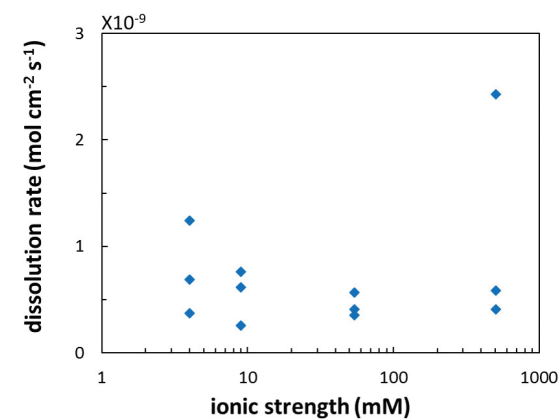


Figure 4 Chemical dissolution rate as a function of ionic strength. The rate is calculated from the AFM height change during the first 30 minutes of flow for regions that underwent dissolution only. The presence of EDTA significantly increases dissolution rates so the results cannot be compared to field rates.



Although we do not observe a connection between grain detachment and salinity in our experiments, it has been shown that brittle rock strength, which is also related to repulsive forces (Røyne *et al.*, 2015), is affected by the concentration of dissolved ions. Rostom *et al.* (2013) showed that at low ionic strength, calcite becomes 20 % weaker relative to its strength in deionised water; at high ionic strength (>1 M) calcite becomes 30 % stronger. While NaCl solutions can impact rock strength, other ion pairs could have a different effect (Bergsaker *et al.*, 2016). Thus, by increasing salinity or in the presence of other ionic species, a stronger impact on grain detachment might be observed.

Conclusions

We have shown that micrometre-sized grains detach from limestone surfaces under stagnant conditions, demonstrating that shear forces are not necessary to account for particle removal. Therefore, grain detachment is expected to occur in carbonate rocks exposed to reactive fluids under field conditions, even when there is little or no flow. Based on the range of hydraulic conductivities for limestone formations (Hiscock, 2005), interstitial velocity in many carbonate aquifers is expected to be low, ranging from 10^{-9} to 10^{-6} m s⁻¹. As long as the fluids in such systems are reactive, a significant flux of calcium carbonate grains could enter the fluid phase as colloidal particles. Although particles released within the pore network of carbonate rocks are expected to be transported only short distances before being immobilised or dissolved, particles detached from fracture surfaces could have much greater mobility.

While grain detachment and movement can occur naturally, these processes could be enhanced during carbon sequestration in formations containing carbonate minerals or during the injection of saline or acidic fluids in enhanced oil recovery. At present, geochemical models do not account for the release and transport of carbonate particles, potentially affecting the prediction of solute transport and evolving porosity and permeability. Although our results suggest that including grain detachment could improve the accuracy of water–rock simulations in carbonate formations, determining if this mechanism is commonplace in other types of carbonate rocks remains a question for the future.

Acknowledgements

We are grateful for financial support from the Israel Science Foundation and the CAMBR fellowship. We also thank two anonymous reviewers and the editor for their constructive comments.

Editor: Susan Stipp

Additional Information

Supplementary Information accompanies this letter at www.geochemicalperspectivesletters.org/article1714

Reprints and permission information are available online at <http://www.geochemicalperspectivesletters.org/copyright-and-permissions>

Cite this letter as: Levenson, Y., Emmanuel, S. (2017) Repulsion between calcite crystals and grain detachment during water–rock interaction. *Geochem. Persp. Let.* 3, 133–141.

References

- BERGSAKER, A.S., RØYNE, A., OUGIER-SIMONIN, A., AUBRY, J., RENARD, F. (2016) The effect of fluid composition, salinity, and acidity on subcritical crack growth in calcite crystals. *Journal of Geophysical Research: Solid Earth* 121, 1631–1651.
- BUHMANN, D., DREYBRODT, W. (1987) Calcite dissolution kinetics in the system H₂O–CO₂–CaCO₃ with participation of foreign ions. *Chemical Geology* 64, 89–102.
- COOPER, T.P., O'BRIEN, P.F., JEFFREY, D.W. (1992) Rates of deterioration of Portland limestone in an urban environment. *Studies in Conservation* 37, 228–238.
- EMMANUEL, S., LEVENSON, Y. (2014) Limestone weathering rates accelerated by micron-scale grain detachment. *Geology* 42, 751–754.
- EMMANUEL, S., ANOVITZ, L.M., DAY-STIRRAT, R.J. (2015) Effects of Coupled Chemo-Mechanical Processes on the Evolution of Pore-Size Distributions. *Reviews in Mineralogy and Geochemistry* 80, 45–60.
- FORD, D., WILLIAMS, P. (2007) *Karst Hydrogeology and Geomorphology*. John Wiley & Sons Ltd, Chichester.
- FREDD, C.N., FOGLER, H.S. (1998) The Influence of Chelating Agents on the Kinetics of Calcite Dissolution. *Journal of Colloid and Interface Science* 204, 187–197.
- GLEDHILL, D.K., MORSE, J.W. (2006) Calcite dissolution kinetics in Na–Ca–Mg–Cl brines. *Geochimica et Cosmochimica Acta* 70, 5802–5813.
- HISCOCK, K.M. (2005) *Hydrogeology: Principles and Practice*. Blackwell Publishing, Malden, Oxford, Carlton.
- LEVENSON, Y., EMMANUEL, S. (2016) Quantifying micron-scale grain detachment during weathering experiments on limestone. *Geochimica et Cosmochimica Acta* 173, 86–96.
- LOMBOY, G., SUNDARARAJAN, S., WANG, K., SUBRAMANIAM, S. (2011) A test method for determining adhesion forces and Hamaker constants of cementitious materials using atomic force microscopy. *Cement and Concrete Research* 41, 1157–1166.
- LUQUOT, L., RODRIGUEZ, O., GOUZE, P. (2014) Experimental characterization of porosity structure and transport property changes in limestone undergoing different dissolution regimes. *Transport in Porous Media* 101, 507–532.
- MORSE, J.W., ARVIDSON, R.S. (2002) The dissolution kinetics of major sedimentary carbonate minerals. *Earth-Science Reviews* 58, 51–84.
- MORSE, J.W., ARVIDSON, R.S., LÜTTGE, A. (2007) Calcium carbonate formation and dissolution. *Chemical Reviews* 107, 342–381.



- NARA, Y., NAKABAYASHI, R., MARUYAMA, M., HIROYOSHI, N., YONEDA, T., KANEKO, K. (2014) Influences of electrolyte concentration on subcritical crack growth in sandstone in water. *Engineering Geology* 179, 41–49.
- OELKERS, E.H., GOLUBEV, S.V., POKROVSKY, O.S., BÉNÉZETH, P. (2011) Do organic ligands affect calcite dissolution rates? *Geochimica et Cosmochimica Acta* 75, 1799–1813.
- ROSTOM, F., RØYNE, A., DYSTHE, D.K., RENARD, F. (2013) Effect of fluid salinity on subcritical crack propagation in calcite. *Tectonophysics* 583, 68–75.
- RØYNE, A., DALBY, K.N., HASSENKAM, T. (2015) Repulsive hydration forces between calcite surfaces and their effect on the brittle strength of calcite-bearing rocks. *Geophysical Research Letters* 42, 4786–4794.
- RUIZ-AGUDO, E., KOWACZ, M., PUTNIS, C.V., PUTNIS, A. (2010) The role of background electrolytes on the kinetics and mechanism of calcite dissolution. *Geochimica et Cosmochimica Acta* 74, 1256–1267.
- VLEUGELS, G., VAN GRIEKEN, R. (1995) Suspended matter in run-off water from limestone exposure setups. *Science of the Total Environment* 170, 125–132.

■ Repulsion between calcite crystals and grain detachment during water–rock interaction

Y. Levenson¹, S. Emmanuel^{1*}

■ Supplementary Information

The Supplementary Information includes:

- Table S-1
- Figures S-1 and S-2

Table S-1 Summary of the experimental conditions and the main results.

Exp. number	[NaCl] (mM)	pH	dissolution rate ^a (mol cm ⁻² s ⁻¹)	detachment ^b (events hr ⁻¹)
1	0	4.8	3.7 × 10 ⁻¹⁰	3.8
2	0	4.8	1.2 × 10 ⁻⁹	2.7
3	0	4.8	6.9 × 10 ⁻¹⁰	2
4	5	4.9	7.6 × 10 ⁻¹⁰	4
5	5	4.9	2.6 × 10 ⁻¹⁰	6.8
6	5	4.9	6.2 × 10 ⁻¹⁰	3
7	50	5.1	3.6 × 10 ⁻¹⁰	3.5
8	50	5.1	4.1 × 10 ⁻¹⁰	2
9	50	5.1	5.7 × 10 ⁻¹⁰	1.8
10	500	4.7	2.4 × 10 ⁻⁹	1.3
11	500	4.7	4.1 × 10 ⁻¹⁰	3.8
12	500	4.7	5.9 × 10 ⁻¹⁰	4.3

^a Mean dissolution rate during the first flow calculated from the AFM height data.

^b Average frequency of grain detachment events during the periods of no-flow

1. Institute of Earth Sciences, The Hebrew University of Jerusalem, Edmond J. Safra Campus, Givat Ram, Jerusalem 91904, Israel

* Corresponding author (email: simonem@cc.huji.ac.il)



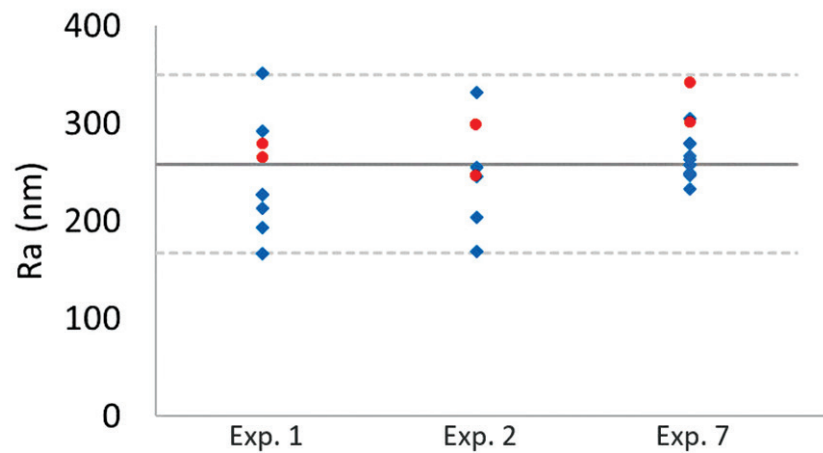


Figure S-1 Results of roughness measurements for three experiments. After the experiments were terminated we measured the roughness of two $10\ \mu\text{m} \times 10\ \mu\text{m}$ regions within the area that been scanned continually during the experiment (red circles) and five to ten additional $10\ \mu\text{m} \times 10\ \mu\text{m}$ regions that had not been previously scanned (blue diamonds). The solid line represents the mean value while the dashed lines represent two standard deviations from the mean value. The roughness average (Ra) is the arithmetic average of the absolute values of the profile height deviations from the mean surface (Z_i) and is calculated according to the equation: $R_a = \frac{1}{n} \sum_{i=1}^n |Z_i|$ where n is the number of pixels in each scan.

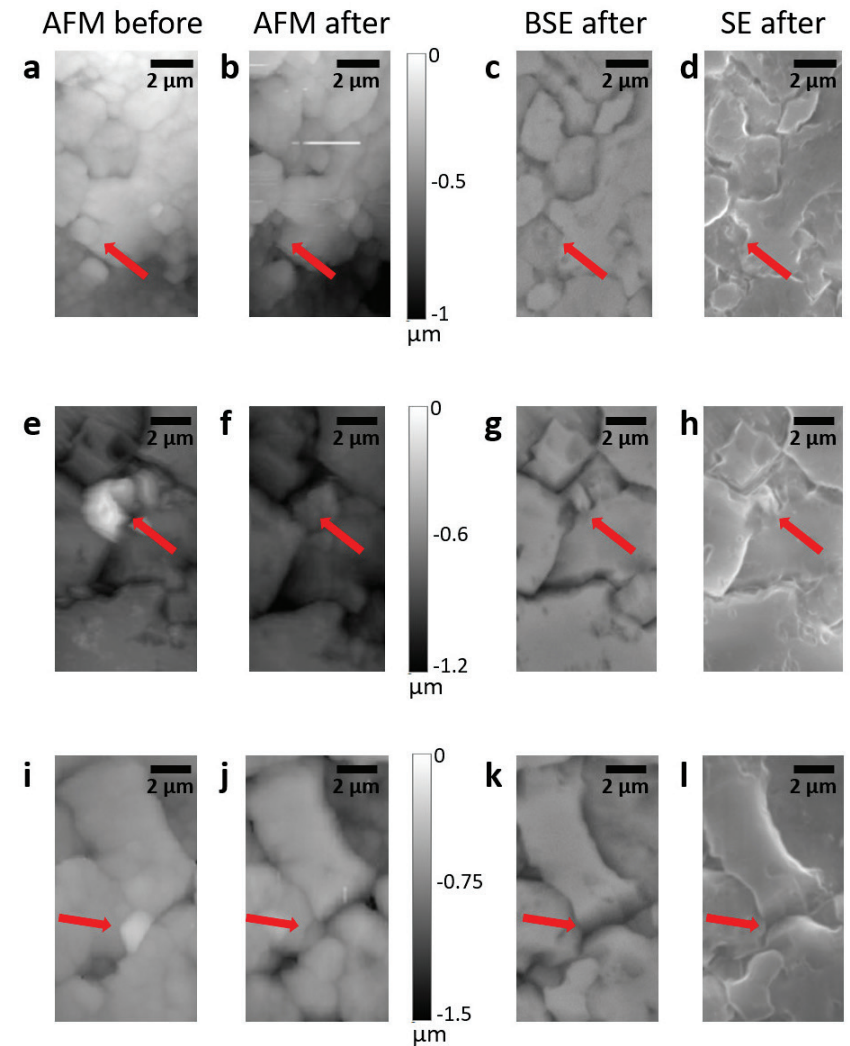


Figure S-2 Grain detachment events during zero flow conditions. In these experiments, the surface of the limestone was imaged with the AFM at the beginning of a period of zero flow. After an hour of no flow, the experiment was terminated and imaged with environmental scanning electron microscopy (ESEM), and then scanned again with AFM under dry conditions. Each row of images represents a comparison of the topography at the beginning of the period of zero flow (a, e, i) with the topography after the experiment was terminated (b, f, j). Backscattered electron (c, g, k) and secondary electron (d, h, l) ESEM images are also shown. Grains present at the beginning of the period of zero flow (indicated by the red arrows) are absent from both the ESEM and AFM image taken after the experiment was terminated. The experiments were carried out with 2 mM EDTA solution without NaCl.

